10.1109/ULTSYM.2014.0592

Accurate diagnosis of nonalcoholic fatty liver disease in human participants *via* quantitative ultrasound

Michael P. Andre[1,2], Aiguo Han[3], *Student Member, IEEE*, Elhamy Heba[1], Jonathan Hooker[1], Rohit Loomba[4], Claude B. Sirlin[1], John W. Erdman, Jr.[5], William D. O'Brien, Jr.[3], *Life Fellow, IEEE*

[1]Department of Radiology, University of California at San Diego, San Diego, CA, [2]San Diego VA Healthcare System, San Diego, CA, [3]Department of Electrical and Computer Engineering, University of Illinois at Urbana-Champaign, Urbana, IL, [4]NAFLD Translational Research Unit, Division of Gastroenterology, Department of Medicine, University of California at San Diego, La Jolla, CA, [5]Department of Food Science and Human Nutrition, University of Illinois at Urbana-Champaign, Urbana, IL; email: wdo@uiuc.edu

Abstract — **Nonalcoholic fatty liver disease (NAFLD) is the most common cause of chronic liver disease in the United States, affects 30% of adult Americans, may progress to nonalcoholic steatohepatitis (NASH) and end-stage liver disease, and is a risk factor for diabetes and cardiovascular disease. The diagnosis, grading, and staging of NAFLD currently is based on liver biopsy examination with histologic assessment. Noninvasive image-based methods to evaluate the liver in adults with NAFLD are urgently needed. We developed a quantitative ultrasound (QUS) method that in animal studies shows promise for detection and quantification of liver fat content. The current study's contribution is to extend the work to human participants by assessing the accuracy of backscatter coefficient and attenuation coefficient for detection of hepatic steatosis in a cohort of adult participants with NAFLD and non-NAFLD controls. QUS parameters measured using routine clinical US scanners show promise for detecting and perhaps grading NAFLD.**

I. Introduction

Nonalcoholic fatty liver disease (NAFLD) is the most common cause of chronic liver disease in the United States, affects 30% of adult Americans, may progress to nonalcoholic steatohepatitis (NASH) and end-stage liver disease, and is a risk factor for diabetes and cardiovascular disease [1]. The diagnosis, grading, and staging of NAFLD currently is based on liver biopsy with histologic analysis. Noninvasive image-based methods to evaluate the liver in adults with NAFLD are urgently needed. Currently, the most accurate and precise noninvasive imaging method for diagnosis and quantification of hepatic steatosis is MRI, which estimates the proton-density fat fraction (PDFF) as a measure of fractional fat content. Although conventional ultrasonography (US) with qualitative interpretation by radiologists is widely used for hepatic steatosis assessment, it is inaccurate. The objective of this study is, using MRI-PDFF as reference, to assess the accuracy for steatosis detection in humans of two quantitative US (QUS) parameters - backscatter coefficient and attenuation coefficient - derived from radiofrequency (RF) signals using the calibrated reference phantom technique [2].

II. QUS Methodology

In order to estimate the attenuation coefficient and backscatter coefficient of human liver tissue *in vivo*, the same transducer (Siemens S3000 with 4C1 transducer; nominal center frequency 3 MHz) and the same settings are used to acquire backscattered signals from each participant's liver and from a homogeneous and calibrated reference phantom whose attenuation and backscatter have been well characterized and known *a priori*. The recorded RF raw data are initially recorded in .rfd format on the Siemens S3000, and are transferred to a PC for offline processing *via* the Ultrasound Research Interface. The .rfd format is converted into .mat format in MATLAB (The MathWorks, Natick, MA) to allow for further processing using a MATLAB-based graphical user interface (GUI) that incorporates the routines for attenuation coefficient and backscatter coefficient estimation from RF data of the tissue and reference phantom.

The attenuation coefficient is estimated from the ultrasonic backscattered RF data using the spectral difference reference phantom method [2]. This frequency-domain method uses the difference in the spectral amplitude at increasing depths to estimate local attenuation from ultrasonic backscatter data. Assuming that the tissue within a small region of interest (denoted sub-ROI) is homogeneous and isotropic, the attenuation coefficient (denoted ATN in dB/cm; later AC will be used to denote the attenuation coefficient in dB/cm-MHz) of the tissue can be estimated at each frequency component from

$$\alpha_s(f) = \alpha_r(f) - \frac{\gamma(f)}{4 \times 8.686} \quad (1)$$

where $\alpha_s(f)$ is the ATN of the tissue sample, $\alpha_r(f)$ is the ATN of the reference phantom, and $\gamma(f)$ is the slope of the straight line that fits the natural log ratio of tissue sample power spectrum to the reference phantom power spectrum as a function of depth.

To implement the algorithm computationally, a Field of Interest (FOI) in the B-mode image of the liver is manually segmented to avoid vessels, lesions, and organ edges. The

segmented area is analyzed to yield ATN (and thereafter the backscatter coefficient) estimates as described below.

The manually drawn FOI is subdivided into many overlapping, rectangular sub-ROIs, each of which yields an estimate of ATN versus frequency. Each individual sub-ROI is subdivided into overlapping axial sections to obtain the power spectrum at different depths through the sub-ROI, a requirement of the spectral difference method. The power spectrum at each depth within each sub-ROI is calculated by gating with a rectangular window, zero-padding to a length of 8192 points (at a sample frequency of 40 MHz), and computing a fast Fourier transform. Averaging the power spectra at a particular depth over all scan lines in the sub-ROI yields the power spectral estimate of the liver tissue for that depth. The same algorithm is repeated automatically on each portion of the reference phantom with the same depth as each corresponding axial section through each corresponding sub-ROI of the liver tissue to obtain the power spectral estimate of the reference phantom. After the power spectra of the participant's liver and the reference phantom are estimated at each depth, ATN is estimated using Equation (1) for the sub-ROI. ATN estimates from all of the sub-ROIs are averaged together to obtain the mean ATN versus frequency over the system's bandwidth 1.7-4.0 MHz. Also, the mean ATN versus frequency curve is fit to the power law form to provide an ATN value for an arbitrary frequency for attenuation compensation during backscatter coefficient estimation.

The size of the sub-ROI for ATN estimation was 24 × 24 mm, and the length of the rectangular gating function was 8.4 mm. These dimensions yield sub-ROIs that are about 20 pulse lengths axially and laterally, as well as a gate length of 7 pulse lengths. The size of the sub-ROI and the length of the axial sections were chosen according to previous findings using simulated RF echo data [3], [4]. The sub-ROI overlap was set to 50% in the axial and lateral directions.

The BSC (backscatter coefficient) estimates were obtained using the reference phantom method [2]. The BSC of the sample can be estimated by

$$BSC_s(z,f) = \frac{S_s(z,f)}{S_r(z,f)} BSC_r(z,f) 10^{2z[\alpha_s(f)-\alpha_r(f)]/10} \quad (2)$$

where BSC_s and BSC_r are the BSCs of the sample and reference phantom, respectively; S_s and S_r are the power spectra for the sample and reference phantom, respectively; z is the depth. The term $10^{2z[\alpha_s(f)-\alpha_r(f)]/10}$ compensates for attenuation effects; note that α_s and α_r are in dB/cm for this form of compensation. The assumptions for Equation (2) are that the transducer surface is touching the abdominal wall of the participant and reference phantom when the scans are being performed, and that the ATN is homogenous in the liver tissue and the reference phantom for attenuation compensation purposes.

To implement the BSC estimation algorithm, the same FOI manually segmented for ATN estimation in each image is used. The FOI is divided into 75%-overlapped sub-ROIs with dimensions 8.93 x 8.93 mm (equivalent to 15 x 15 wavelengths at 2.5 MHz). The power spectrum of each sub-ROI is calculated by gating with a Hanning window and computing a fast Fourier transform of each gated A-line in the sub-ROI. Averaging the power spectra over all A-lines in the sub-ROI yields the power spectral estimate of the liver tissue for that sub-ROI. The same algorithm is repeated automatically on each portion of the reference phantom with the same depth as each corresponding sub-ROI of the liver tissue to obtain the power spectral estimate of the reference phantom. With the estimated power spectra of both the liver tissue and the reference phantom, the BSC of the sub-ROI can be estimated using Equation (2). BSC estimates from all the sub-ROIs are averaged together to obtain the mean BSC versus frequency over the bandwidth 2.0-4.0 MHz. The lower end of the frequency range is limited to 2.0 MHz because the BSC of the reference phantom is accurately characterized down to 2.0 MHz.

III. Statement of Contribution

This is an IRB-approved, HIPPA compliant study. We developed a novel QUS method that in animal studies shows promise for detection and quantification of liver fat content. The current study's contribution is to extend the work to human participants by assessing the accuracy of the backscatter coefficient and the attenuation coefficient for detection of hepatic steatosis in a cohort of adult participants with NAFLD (defined as MRI-PDFF ≥ 5%) and negative controls (defined as MRI-PDFF < 5%). Same-day liver MRI and US exams were performed using routine clinical scanners, from which MRI-PDFF and both model-free QUS parameters (BSC and AC) were estimated. Sensitivity and specificity were calculated for BSC and AC using MRI-PDFF ≥ 5% as the diagnostic threshold.

IV. Results and Discussion

One hundred six adult research participants with known or suspected NAFLD were prospectively enrolled including 61 who had NAFLD (defined as MRI-PDFF ≥ 5%) and 45 who did not have NAFLD, and classified as non-NAFLD controls (MRI-PDFF < 5%). Fig 1 shows the AC (dB/cm-MHz) at 3.0 MHz as a function of the MRI-PDFF for the 106 participants. A power-law fit between AC and MRI-

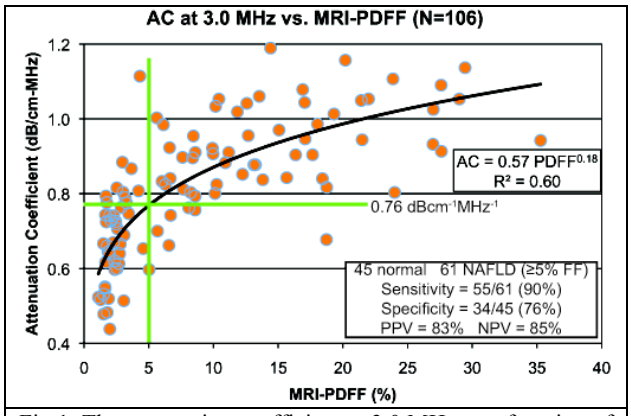

Fig 1. The attenuation coefficient at 3.0 MHz as a function of MRI PDFF. The green vertical line denotes 5% MRI-PDFF (the NAFLD diagnostic threshold) that intercepts the power-law fit at 0.76 dB/cm-MHz.

PDFF yielded AC = 0.57 PDFF$^{0.18}$ (R^2 = 0.60); at MRI-PDFF = 5% (diagnostic threshold for NAFLD), AC = 0.76 dB/cm-MHz. The AC cutoff value of 0.76 dB/cm-MHz provided a raw sensitivity of 90% and specificity of 76% for the diagnosis of NAFLD.

Fig 2 shows the BSC as a function of the MRI-PDFF for the 106 participants. A power-law fit between BSC and MRI-PDFF yielded BSC = 0.00022 PDFF$^{1.55}$ (R^2 = 0.74); at MRI-PDFF = 5% (diagnostic threshold for NAFLD), BSC = 0.0027 1/cm-sr. The BSC cutoff value of 0.0027 1/cm-sr provided a raw sensitivity of 95% and specificity of 96% for the diagnosis of NAFLD.

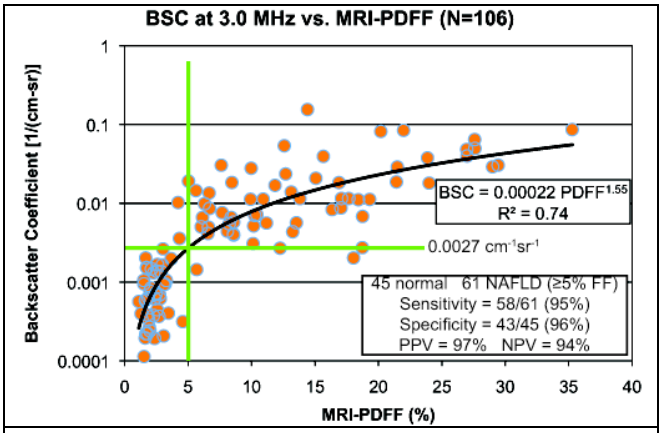

Fig 2. The backscattered coefficient at 3.0 MHz as a function of MRI PDFF. The green vertical line denotes 5% MRI-PDFF (the NAFLD diagnostic threshold) that intercepts the power-law fit at 0.0027 1/cm-sr.

Fig 3 shows the AC vs. BSC, both at 3.0 MHz, for the 106 participants. The data are segmented into three MRI-PDFF ranges: <5.0%, 5.0-12.5%, and > 12.5%. It can be observed that the majority of the 45 (37/45 = 82%) negative controls (MRI-PDFF < 5%) appear in the lower left quadrant (relative to the two green lines) and a majority of the 61 (52/61 = 85%) NAFLD participants (MRI-PDFF ≥ 5%) appear in the upper right quadrant.

V. Conclusion

QUS parameters measured using routine clinical US scanners show promise for diagnosing and perhaps grading NAFLD.

Acknowledgments

The authors would like to thank Jamie Kelly and Nick Olsen from the University of Illinois at Urbana-Champaign for their valued assistance.

The development of the GUI used to process the quantitative ultrasound data was supported, in part, by NIH R01CA111289. The use of the Siemens S3000 scanner was loaned to UCSD under a research agreement with Siemens Medical Systems, Inc.

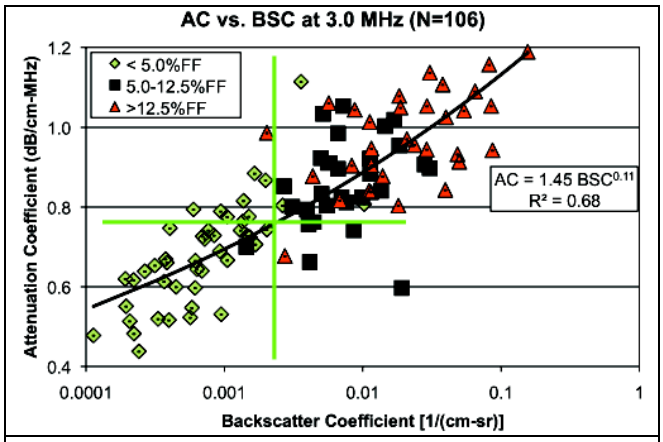

Fig 3. The attenuation coefficient as a function of backscattered coefficient at 3.0 MHz for which the data are identified in three MRI-PDFF ranges. The green horizontal and vertical lines denote AC and BSC cutoff values corresponding to 5% MRI-PDFF in Fig 1 (AC) and Fig 2 (BSC), respectively.

References

[1] Charlton M, Krishnan A, Viker K, Sanderson S, Cazanave S, McConico A, Masuoko H, Gores G. The fast food diet mouse: novel small animal model of NASH with ballooning, progressive fibrosis and high physiologic fidelity to the human condition. American Journal of Physiology. Gastrointestinal and Liver Physiology, 30; G825-34. Epub, Aug 11, 2011.

[2] Yao LX, Zagzebski JA, Madsen EL. Backscatter coefficient measurements using a reference phantom to extract depth-dependent instrumentation factors. Ultrasonic Imaging, 12, 58-70, 1990.

[3] Labyed Y. Optimization and application of ultrasound attenuation estimation algorithms, PhD dissertation, Iowa State University, 2011.

[4] Labyed Y, Bigelow TA, McFarlin BL. Estimate of the attenuation coefficient using a clinical array transducer for the detection of cervical ripening in human pregnancy. Ultrasonics, 51, 34-39, 2011.